CHEMISTRY
A EUROPEAN JOURNAL

DOI: 10.1002/chem.200701029

Conformational Preference and Potential Templates of *N*-Methylated Cyclic Pentaalanine Peptides

Jayanta Chatterjee,[a] Dale F. Mierke,[b] and Horst Kessler*[a]

Abstract: Systematic *N*-methylation of all peptide bonds in the cyclic pentapeptide cyclo(-D-Ala-Ala_4-) has been performed yielding 30 different *N*-methylated derivatives, of which only seven displayed a single conformation on the NMR time scale. The conformation of these differentially *N*-methylated peptides was recently reported by us (*J. Am. Chem. Soc.* **2006**, *128*, 15164–15172). Here we present the conformational characterization of nine additional *N*-methylated peptides from the previous library which are not homogeneous but exist as a mixture in which at least one conformation is preferred by over 80%. The structures of these peptides are investigated employing various 2D-NMR techniques, distance geometry calculations and further refined by molecular dynamics simulations in explicit DMSO. The comparison of the conformation of these nine peptides and the seven conformationally homogeneous peptides allow us to draw conclusions regarding the influence of *N*-methylation on the peptide backbone of cyclic pentapeptide of the class cyclo(-D-Ala-Ala_4-). Here we present the different conformational classes of the peptides arising from the definitive pattern of *N*-methylation which can eventually serve as templates for the design of bioactive peptides.

Keywords: conformation analysis · peptides · template structures

Introduction

The conformation of cyclic peptides of smaller ring size (e.g., five to seven-membered rings) is mainly determined by the array of chirality of the amino acids in the peptide sequence.[1] Hence, such peptides which consist only of D- and L-alanine can be used as templates for designing distinct peptide conformations containing any of the other natural amino acids, with the exception of glycine and proline. This concept has been employed to establish scaffolds for "spatial screening" and for the design of bioactive peptides.[2] Another dimension to each of these scaffolds is provided by *N*-methylation[3–5] as it introduces remarkable changes in the backbone constitution and conformation of cyclic peptides.[4] The changes in the backbone conformation influence the biological activity and selectivity of peptidic ligands.[5] *N*-Methylation affects the conformation of the modified amino acid as well as the preceding residue.[6] In addition it facilitates the occurrence of a *cis*-peptide bond which, in comparison to the *trans*-peptide bond, is thermodynamically less unfavored than the secondary amide bond.[7] In case of cyclic peptides *N*-methylation has further long-range impact on the entire backbone conformation. *N*-Methylation affects the backbone of the peptide by reducing the number of hydrogen-bond donors preventing intramolecular and intermolecular hydrogen bonding, and potentially enhances the pharmacokinetic properties of the peptide by blocking the proteolytic cleavage sites.[8] The presence of *N*-methyl backbone groups also increases the hydrophobicity of the peptide bond and, consequently, its ability to interact more selectively with the complementary hydrophobic pocket along with enhanced the membrane permeability.[9] The usual approach to search for selective and potent peptide ligands is the "*N*-methyl scan", wherein a library of all available sites of peptide bonds consecutively are *N*-methylated.[10] So far "*N*-methyl scans" have been used almost exclusively to introduce only a single *N*-methylated peptide bond per molecule.[5,8,11] In our attempt to improve the bioavailability we introduce libraries including poly-*N*-methylated peptides.

With the conformational preference of all possible combinations of *N*-methylated analogues defined, those which

[a] M. Sc. J. Chatterjee, Prof. Dr. H. Kessler
Center for Integrated Protein Science at the
Department Chemie, Lehrstuhl für Organische Chemie II
Technische Universität München, Lichtenbergstrasse 4
85747 Garching (Germany)
Fax: (+49) 89-298-13210
E-mail: horst.kessler@ch.tum.de

[b] Prof. Dr. D. F. Mierke
Department of Chemistry, Dartmouth College
Hanover, NH 03755 (USA)

Supporting information for this article is available on the WWW under http://www.chemeurj.org/ or from the author.

adopt a distinct structure can be employed as templates. It is thus possible to design a desired conformation of a peptide sequence without the requirement of synthesizing and screening a large library of derivatives.

In the search of highly conformationally preferred cyclic *N*-methylated peptides derived from cyclo(-D-Ala-Ala_4-), abbreviated as c(aA_4), (we use the abbreviation "a" for D-Ala and "A" for L-Ala), we identified seven peptides in which less than 2% of a second conformation is found.[1c] These seven examples represent ideal structural templates; however, there are several others which show one or more conformations in an amount lower than 20%. We anticipate that also these peptides could also be applied as conformational templates, especially if they exhibit new conformational types which were not found in the seven homogeneous peptides. Here we present the conformation of the additional nine peptides, which prefer one conformation by more than 80%.

Results

The combinatorial manner to illustrate the entire library is shown in Figure 1. Given five amide bonds there is the possibility of 31 (2^5-1) differently *N*-methylated cyclic derivatives of c(aA_4). We were able to synthesize all but the permethylated derivative. The NMR-based analysis of the thirty compounds displayed various populations of major and minor conformers slowly interconverting on the NMR time scale. For use as templates in rational drug design we are mainly interested in those peptides which prefer a single conformation of greater than 80%. As a first pass, we examined the seven conformationally homogeneous (>98%) cyclic peptides.[1c] Herein, we present the results from the nine compounds that have a major conformation of between 80–98%, and then the complete characterization of all sixteen conformationally abundant cyclic peptides from this library.

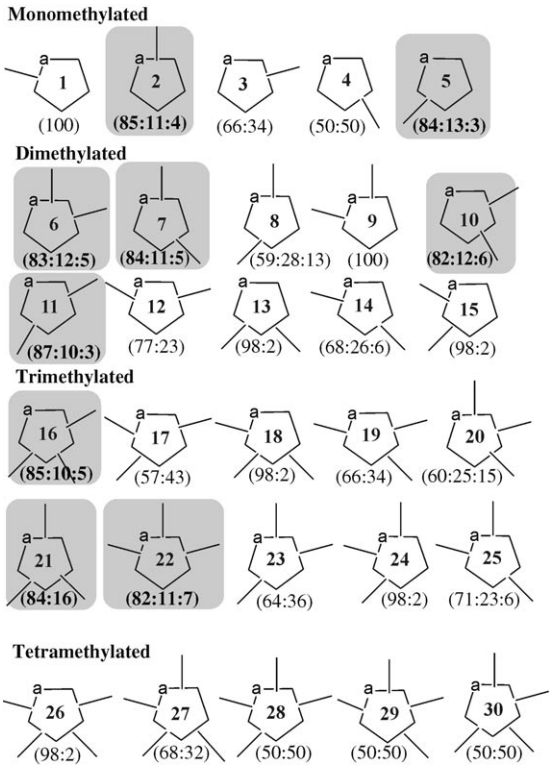

Figure 1. Library of all the synthesized *N*-methylated cyclic pentapeptides with their conformational abundance of the NMR time shift scale in parenthesis. The peptide sequence follows the convention and is to read clock-wise. The nine peptides shaded in gray are described here. Each vertex of the pentagon represents L-alanine and the edges representing the peptide bond. *N*-Methylation is represented by lines and belongs to the following residue (vertex) going in a clockwise manner. The D-alanine is represented by the small letter "a".

It is essential to note that in these small cyclic peptides, the conformation is strongly dependent on steric interactions rather than on internal hydrogen bonds, which was well documented over a quarter of a century ago.[12] This is in contrast to standard discussions on cyclic peptide conformations which often are claimed to be "stabilized" by intramolecular hydrogen bonds. In our *N*-methylated cyclic pentapeptides we rarely observe "classical" β or γ turns. It is well known that inter- or intramolecular hydrogen bonds shift the amide proton NMR signal downfield. In DMSO, NH protons exposed to the solvent exhibit a distinct downfield shift by binding to the strongly basic sulfoxide group of the solvent. Intramolecularly oriented NH groups even when involved in hydrogen bridges to amide carbonyls are shifted upfield and show small temperature gradients. Temperature gradients of protons which bind solvent molecules are large, indicating entropy driven hydrogen bond breaking at higher temperatures.[1a]

Conformation of nine cyclic peptides

cyclo(-D-Ala^1-$MeAla^2$-Ala^3-Ala^4-Ala^5-) (2): This compound is *N*-methylated at Ala^2 and contains a *cis*-peptide bond in the minor conformation. The analysis of the major conformation exhibits no defined classical turn structure (Figure 2). The strong preference of a βII′ turn around the D-Ala^1-$MeAla^2$ bond obviously is overcome by the *N*-methylation. The *N*-methyl group is pointing slightly inside the ring. It is remarkable that all *Φ* angles are adjusted to fulfill the *syn* orientation of the α CH bond and the carbonyl bond of the preceding amino acid. Obviously this orienta-

Figure 2. Stereopicture of cyclo(-D-Ala^1-$MeAla^2$-Ala^3-Ala^4-Ala^5-) (**2**). An energy minimized average of trajectory of 150 ps free MD in explicit solvent DMSO is shown.

tion is so strongly preferred energetically,[13] that other conformations cannot compete and the amount of the minor populated conformations is only 15%. Compound **2** exhibit a structure where three adjacent NH groups point to the same side of the molecule (upwards). Such a structure nicely exhibits that the formation of intramolecular hydrogen bonds are not essential for a preferred backbone conformation in cyclic peptides.[12]

The experimental $^3J(H^N,H^\alpha)$ coupling constant of D-Ala^1 is 6.2 Hz, however, the dihedral angle calculated by averaging the dihedral angle of all the structures in the trajectory (a structure was written to the trajectory every femtosecond, resulting in 1500 structures) between D-Ala^{1}H$^\alpha$ and H^N is −14.6° which would have resulted in a coupling constant of 8.2 Hz.[14] As the peptide does not show any major violation of the ROE values (all ROEs are fulfilled within 0.1 Å) we assume that the coupling constant indicates a flip of peptide bond plane (Ala^5–D-Ala^1) about the adjacent Φ and Ψ. The substitution pattern corresponds to the structure of Cilengitide [cyclo(-RGDfNMeVal-)],[5b] with one distinct difference: Ala^4 of **2** is substituted by a glycine in Cilengitide, which allows more flexibility for the RGD peptide. In general both peptides exhibit similar structures[5c] confirming our premise that the conformation of small cyclic peptides in the first approximation is determined by the sequence of the chiralities of the amino acid sequence. However, it should be kept in mind that the functional group of the amino acid side chains may affect the backbone conformation mainly with respect to the conformational homogeneity on the NMR time scale, though the backbone conformation is expected to show the same pattern of *cis* and *trans* peptide with similar Φ and Ψ compared with the model alanine peptides described herein.

cyclo(-D-Ala^1-Ala^2-Ala^3-Ala^4-MeAla^5-) (5): The compound obtained by *N*-methylation of the parent c(aA$_4$) at Ala^5 (Figure 3), contains only *trans* peptide bonds. There are no

Figure 3. Stereopicture of cyclo(-D-Ala^1-Ala^2-Ala^3-Ala^4-MeAla^5-) (**5**) (details in Figure 2).

major violations of the ROE values in the structure. The strong ROEs between Ala^{5}N^{Me}–Ala^{5}H$^\alpha$, Ala^{5}N^{Me}–Ala^{4}H$^\alpha$, and Ala^{5}N^{Me}–D-Ala^{1}H^N define the spatial arrangement of the *N*-methyl group, which is pointing down from the plane of the peptide cycle. Most of the Φ angles are close to the preferred −120° except in position 5, where the *N*-methyl group avoids steric clash with the two side chain methyl groups of Ala^4 and Ala^5.

cyclo(-D-Ala^1-MeAla^2-MeAla^3-Ala^4-Ala^5-) (6): The NMR spectrum of the preferred conformation shows a strong ROE between Ala^{2}H$^\alpha$ and Ala^{3}H$^\alpha$, indicating the presence of an Ala^2–Ala^3 *cis*-peptide bond. The *cis*-peptide bond (Figure 4) is caused by the strong steric clash between

Figure 4. Stereopicture of cyclo(-D-Ala^1-MeAla^2-MeAla^3-Ala^4-Ala^5-) (**6**) (details in Figure 2). The peptide bond between Ala^4 and Ala^5 flips by about 180° about Φ and Ψ (see text).

Ala^{3}N^{Me} and Ala^{2}N^{Me}. Starting with the conformation of **2** and introduction of the NMe group at the Ala^3 residue (see Figure 2), forces the Ala^2–Ala^3 peptide bond into the *cis* orientation. It is reassuring to observe that the structure from Ala^5 to Ala^2 is identical in **2** and **6**. The *cis*-peptide bond maximizes the distance between the methyl groups. Due to the flip of the Ala^4–Ala^5 peptide bond only three H$^\alpha$ out of five are in the preferred orientation being *syn*-periplanar with the CO of the adjacent residue. On the other hand, the NH of Ala^5 can now form a γ turn by bonding to CO of Ala^3. However, there are several indications that the amide bond Ala^4–Ala^5 flips around as was previously found for the amide bond Ala^3–Ala^4 in c(pA$_4$);[1b,13,15] the temperature gradient (Table 1) of −3.6 ppb per K of Ala^{5}H^N does not indicate a strong solvent shielding of Ala^{5}H^N. The peptide shows strong ROE violation between Ala^{5}H^N–Ala^{4}H^N and Ala^{5}H^N–Ala^{5}H$^\beta$ (0.3 and 0.4 Å, respectively, longer than the experimental values), whereas the strong ROE between Ala^{5}H^N–Ala^{4}H$^\alpha$ is not violated. This is caused by the r^{-6} dependence of the ROE which emphasize small distances and forces the molecule into the conformation shown in Figure 3, whereas the participation of the conformation with the Ala^{5}H^N pointing upwards is not exhibited. The commonly utilized restrained MD does not usually properly present

Table 1. Temperature gradient values of NH protons ($-\Delta\delta$ per ΔT) in ppb K^{-1} and the values in parenthesis are the respective $^3J(H^N,H^\alpha)$ coupling constants in Hz in DMSO.

Peptide	D-Ala^1	Ala^2	Ala^3	Ala^4	Ala^5
2	5.4(6.2)	–	2.6(7.2)	3.0(6.8)	2.0(8.4)
5	5.6(8.4)	1.3(8.2)	3.6(7.6)	1.7(7.0)	–
6	7.5(9.0)	–	–	5.1(8.2)	3.6(7.7)
7	4.3(9.0)	–	4.5(8.3)	–	4.0(8.4)
10	6.0(6.8)	0.6(8.5)	–	–	4.0(7.5)
11	3.7(8.1)	2.4(7.5)	–	4.5(8.0)	–
16	4.0(8.7)	6.0(9.8)	–	–	–
21	4.5(5.8)	–	2.0(7.4)	–	–
22	–	–	–	3.7(9.2)	1.5(9.3)

such rapid conformational equilibria and more sophisticated technologies such as ensemble-based or time-dependent restrained MD methods must be utilized.[16] For our present purposes it is sufficient to be aware of those effects when analyzing peptide conformations.

cyclo(-D-Ala^1-MeAla^2-Ala^3-MeAla^4-Ala^5-) (7): This compound differs from **6** by shifting the -NMe group from Ala^3 to Ala^4. A *cis*-peptide bond is now observed between Ala^3 and Ala^4 in the dominant conformation (Figure 5). On the other hand the structure in the range from Ala^4 to Ala^2 is almost identical in **6** and **7**. The latter is the only compound containing a *cis*-peptide bond at this position. In contrast to **6** there are no ROE violations. All experimental $^3J(H^N,H^\alpha)$ coupling constants are large indicating *syn*- or *anti*-periplanar arrangement of H^N and H^α.

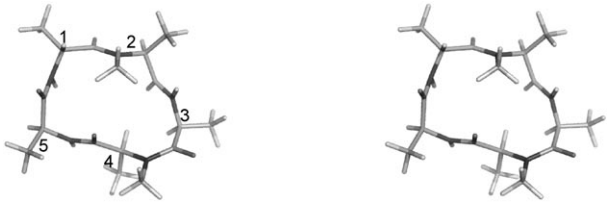

Figure 5. Stereopicture of cyclo(-D-Ala^1-MeAla^2-Ala^3-MeAla^4-Ala^5-) (**7**) (details in Figure 2).

cyclo(-D-Ala^1-Ala^2-MeAla^3-MeAla^4-Ala^5-) (10): The compound is *N*-methylated at Ala^3 and Ala^4. The NMR spectrum of the major conformation shows the absence of any $(i)H^\alpha$–$(i+1)H^\alpha$ ROE cross peak of the major conformer, indicating that all peptide bonds are *trans*. This is surprising because all other peptides which contain an NMeAla^3 exhibit a *cis*-peptide bond at this position. The ROEs did not clearly define the spatial orientation of the *N*-methyl groups. Although the calculation yields a structure with a minor violation, the result is not in agreement with the observation, because we found several missing ROE values which should be present if the calculated structure would be correct. As **10** is not conformationally homogenous and preliminary investigations show that substitution of Ala by Val at different positions does not cause a shift to conformational homogeneity, we will not further discuss this compound here. Usually a substitution of an Ala by Val enhances the conformational homogeneity (the study of these effects is currently ongoing).

cyclo(-D-Ala^1-Ala^2-MeAla^3-Ala^4-MeAla^5-) (11): This compound is obtained by formal *N*-methylation of **5** at Ala^3. Surprisingly this small change induces the peptide bonds between Ala^2–Ala^3 and Ala^4–Ala^5 to adopt the *cis* conformation (Figure 6). This avoids steric interaction of all the methyl groups from Ala^2 to Ala^5. ROE violations are observed only for Ala$^5H^\alpha$–D-Ala$^1H^N$ and Ala$^5H^\beta$–D-Ala$^1H^N$ but the rest of the ROEs are in total agreement to the MD calculations. To explain these ROE violations we assume again that the Ala^5–D-Ala^1 peptide bond is flipping and directs D-Ala^{1}NH above and below the plane.

Figure 6. Stereopicture of cyclo(-D-Ala^1-Ala^2-MeAla^3-Ala^4-MeAla^5-) (**11**) (details in Figure 2).

cyclo(-D-Ala^1-Ala^2-MeAla^3-MeAla^4-MeAla^5-) (16): The compound is obtained by additional *N*-methylation of **11** at Ala^3–Ala^4 peptide bond. Thus the compound has similar structural elements as **11** except the obvious rotation of the Ala^3–Ala^4 peptide bond by about 150° due to the *N*-methylation of the peptide bond (Figure 7). The peptide shows some violations in the ROEs, which again indicates some flexibility of the peptide bonds. There is a typical ROE between D-Ala$^1H^N$–Ala$^3H^\alpha$ which is violated by 0.25 Å; however, the other ROEs of D-Ala$^1H^N$ are not violated. This suggests another orientation of the Ala^5–D-Ala^1 peptide bond than present in the average structure, where D-Ala$^1H^N$ is close to Ala$^3H^\alpha$ formed by an anticlockwise rotation of the Ala^5–D-Ala^1 peptide bond. The Ala$^2H^N$ also shows the following ROE violations Ala$^2H^N$–Ala$^4N^{Me}$, Ala$^2H^N$–Ala$^2H^\beta$, and Ala$^2H^N$–Ala$^3H^\alpha$. The first and the third violations restrict the Ala$^2H^N$ to orient in a fashion so that it points towards Ala$^3H^\alpha$/Ala$^4N^{Me}$ and the second violation restricts the Ala$^2H^N$ to a close proximity to Ala$^2H^\beta$; thus, these two sets of violations in the peptide points towards the flipping of Ala^5–D-Ala^1 and D-Ala^1–Ala^2 peptide bond. From the average structure one might conclude the presence of a γ turn about D-Ala^1; however, the temperature gradient values do not suggest that the Ala$^2H^N$ is solvent shielded.

Figure 7. Stereopicture of cyclo(-D-Ala^1-Ala^2-MeAla^3-MeAla^4-MeAla^5-) (**16**) (details in Figure 2).

cyclo(-D-Ala^1-MeAla^2-Ala^3-MeAla^4-MeAla^5-) (21): Starting from **7**, **21** is formally *N*-methylated at Ala^5. It is evident from Figure 5 that *N*-methylation of Ala^5 is sterically forbidden. In fact, whereas the whole conformation between Ala^5–

Ala^2 is retained in **7** and **21** (Figure 8), there is a change in the *cis*/*trans* arrangement of the peptide bond (*cis*-peptide bond in **7** is between Ala^3–Ala^4, but in **21** between Ala^4–Ala^5) in addition to the backbone conformation in the region Ala^3–Ala^5. The spatial orientation of Ala^{4}N^{Me} is defined by exactly the same ROEs as in **16**. The compound shows a major violation of 0.34 Å of the ROE between Ala^{2}H$^\alpha$ and Ala^{3}H^N. Additionally the Ala^{3}H^N shows a temperature gradient value of -2.00 ppb K^{-1}, suggesting it is solvent shielded. These data are consistent with rapid flipping of the Ala^3–Ala^2 peptide bond. The experimental D-Ala^1 ^3J(H^N,H$^\alpha$) coupling constant of 5.8 Hz is inconsistent with the average structure where the dihedral angle between D-Ala^{1}H$^\alpha$ and D-Ala^{1}H^N is $-4.2°$. This observation is also consistent with the observed minor violations of the ROEs between D-Ala^{1}H$^\alpha$–D-Ala^{1}H^N, D-Ala^{1}H^N–D-Ala^{1}H$^\beta$ and D-Ala^{1}H^N–Ala^{5}H$^\alpha$. These violations suggest an orientation wherein the Ala^5–D-Ala^1 peptide bond is rotated clockwise satisfying the observed ROE violations. However, as this is a sterically demanding situation, the structure relaxes energetically during the free MD run, resulting in the violation of the coupling constants and ROE.

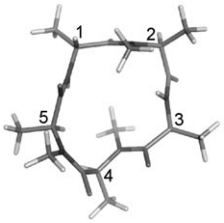

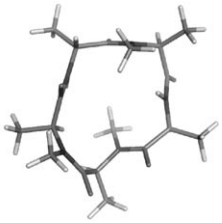

Figure 8. Stereopicture of cyclo(-D-Ala^1-MeAla^2-Ala^3-MeAla^4-MeAla^5-) (**21**) (details in Figure 2).

cyclo(-D-MeAla^1-MeAla^2-MeAla^3-Ala^4-Ala^5-) (22): The compound can be obtained by further *N*-methylation of Ala^5–D-Ala^1 peptide bond of **6**. The compound as one expects from **6**, shows a *cis*-peptide bond about Ala^2–Ala^3 residue whereas all other peptide bonds are in the *trans* configuration (Figure 9). The spatial orientation of D-Ala^{1}N^{Me} is determined by the ROEs Ala^{5}H$^\alpha$–D-Ala^{1}N^{Me} and Ala^{5}H^N–D-Ala^{1}N^{Me}. The deep burying of the Ala^{3}H$^\beta$ is determined by the ROE Ala^{2}H$^\alpha$–Ala^{3}H$^\beta$ interaction. There are no major violations of the ROEs in the calculated structure except the intraresidual ROE between Ala^{5}H^N–Ala^{5}H$^\alpha$ suggesting dynamics of the Ala^4–Ala^5 peptide bond. The compound has similar structural elements as **6** and the *N*-methyl groups are spatially oriented in a fashion to have minimum possible steric clash with the *N*- and β-protons. The low temperature coefficient value of -1.49 ppb K^{-1} for Ala^{5}H^N indicates it is solvent shielded. However, the absence of the ROE between Ala^{5}H^N–Ala^{4}H^N and the absence of any violations, unlike the parent c(aA$_4$), defines the orientation of the Ala^4–Ala^5 peptide bond and suggests the presence of a closed γ turn about Ala^4.

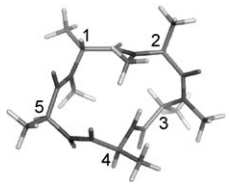

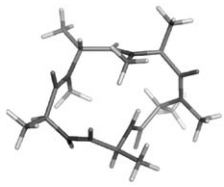

Figure 9. Stereopicture of cyclo(-D-MeAla^1-MeAla^2-MeAla^3-Ala^4-Ala^5-) (**22**) (details in Figure 2).

To summarize the different conformations, the Φ and Ψ values of the different peptides are given in Table 2.

Table 2. Φ and Ψ values of the peptides with a preferred conformation. The Ω values are summarized as *cis* (0°) and *trans* (180°), denoted by c and t, respectively.

No.	D-Ala^1			Ala^2			Ala^3			Ala^4			Ala^5		
	Φ	Ψ	Ω	Φ	Ψ	Ω	Φ	Ψ	Ω	Φ	Ψ	Ω	Φ	Ψ	Ω
2	118	−81	t	−94	−61	t	−87	−66	t	−100	−67	t	−114	82	t
5	129	−94	t	−94	−64	t	−100	−61	t	−112	101	t	66	75	t
6	128	−87	t	−131	74	t	−110	11	c	−99	100	t	56	56	t
7	117	−90	t	−101	−89	t	−126	83	t	−128	−166	c	57	64	t
11	−55	−71	t	−138	79	t	−128	43	c	−138	72	t	−94	−23	c
16	86	−95	t	−134	84	t	−122	149	c	53	61	t	−112	151	c
21	116	−94	t	−80	−48	t	−129	80	t	58	74	t	−116	142	c
22	121	−84	t	−135	80	t	−109	48	c	−138	86	t	54	63	c

Discussion

With the detailed conformational characterization of the eight compounds described here, a total of 15 out of the 30 *N*-methylated alanine peptides, all which prefer one conformation over 80 %, can be analyzed. As a first approach, the peptides can be grouped into five different classes (Figure 10) based on the number and position of the *cis*-peptide bonds. It should also be noted that in these conformationally homogeneous templates, we observe conformational dynamics (i.e., a rotation about Φ and Ψ) about peptide bonds, which are fast on the NMR shift time scale. Those processes are often found in peptides and are detected by non-agreement of observed and calculated distances in distinct areas. Flipping peptide bonds[15] are indicated in bold in Figure 10.

In class I, there are six compounds possessing all-*trans*-peptide bonds. In class II, there are two compounds which have a *cis*-peptide bond between Ala^2–Ala^3, while class III contains three compounds with a single *cis*-peptide bond between Ala^4–Ala^5. Class IV has three compounds with two *cis*-peptide bonds (between Ala^2–Ala^3 and Ala^4–Ala^5) and finally class V has one compound, with a single *cis*-peptide

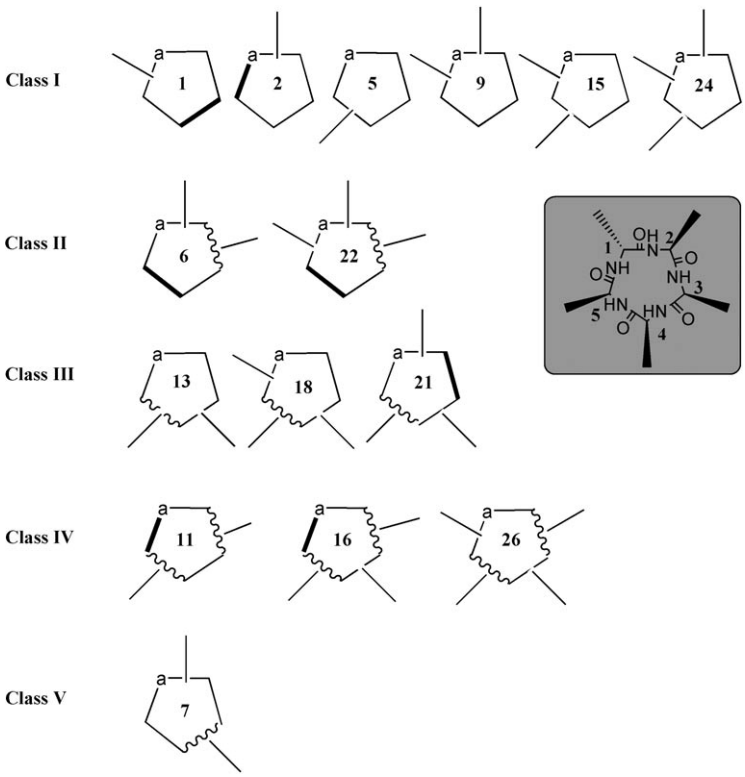

Figure 10. Schematic representation of five different classes of cyclic *N*-methylated(-D-Ala-Ala_4-). The wavy bonds denote the *cis*-peptide bond and the thick bonds denote the flipping nature of the peptide bond. The inset depicts clearly the numbering and stereochemistry of the parent peptide.

bond between Ala^3–Ala^4. Thus combining all the possibilities of the occurrence of the *cis*-peptide bond, one can ascertain that the region between Ala^5 to Ala^3 is highly conserved as under no circumstance is a *cis*-peptide bond about Ala^5–D-Ala^1 and D-Ala^1–Ala^2 observed. The region between Ala^2 to Ala^5 on the other hand is variable, where *N*-methylation of the peptide bond leads to the formation of one, two, or no *cis*-peptide bond varying with the pattern of *N*-methylation. In class II and IV, the compounds have a common *N*-methylated Ala^2–Ala^3 peptide bond leading to the formation of a *cis*-peptide bond in this position, owing to the strong steric interaction with the adjacent β-methyl groups. There is only one compound, that is **7**, which has an *N*-methylated Ala^3–Ala^4 peptide bond in the *cis* conformation. All other peptides, that is, **13**, **16**, **18**, **21**, and **26**, which contain the Ala^3–Ala^4 *N*-methylated peptide bond, exhibit a *trans* conformation. To understand this behavior we begin with **4**, wherein only Ala^4 is *N*-methylated. Here we observe 50:50 equilibrium (Figure 1) of this Ala^3–Ala^4 peptide bond in the *cis* and *trans* conformation (data not shown). *N*-Methylation only at Ala^2 shifts the equilibrium to a strong *cis* preference as in **7** (Figure 1), whereas *N*-methylation at any other sites shifts it to *trans*.

In class III, the three compounds possessing a *cis*-peptide bond at Ala^4–Ala^5 also have the adjacent *trans* Ala^3–Ala^4 peptide bond *N*-methylated. It seems that only the *N*-methylation at the Ala^4–Ala^5 is not sufficient to introduce a *cis*-peptide bond at this position until the previous Ala^3–Ala^4 peptide bond is *N*-methylated (e.g., the mono-methylated compound, **5**, exhibits one abundant *trans* conformer) and all the three compounds, **13**, **18** and **21** have a common *N*-methylated Ala^3–Ala^4 peptide bond. However, similar to the previous case there is an exception to this pattern: peptide **11** where the Ala^4–Ala^5 peptide bond is *cis* despite the absence of the *N*-methylated Ala^3–Ala^4 peptide bond. An explanation of this observation can be extracted after taking all the six compounds into account which have *N*-methylated Ala^4–Ala^5 peptide bond. Here one observes that the single *N*-methylation of Ala^4–Ala^5 peptide bond or in conjunction with *N*-methylated Ala^5–D-Ala^1 and/or D-Ala^1–Ala^2 does not force Ala^4–Ala^5 into the *cis* conformation. Instead when in conjunction with *N*-methylated Ala^2–Ala^3 and Ala^3–Ala^4 peptide bond, the Ala^4-Ala^5 peptide bond eventually orients in a *cis* conformation. Thus, either *N*-methylation of Ala^2–Ala^3, Ala^3–Ala^4 or both is crucial to direct the *N*-methylated Ala^4–Ala^5 peptide bond into *cis* conformation.

In class IV all of the three compounds, **11**, **16** and **26**, have two *cis*-peptide bonds in equivalent positions; all three compounds are identical except for the orientation of the Ala^5–D-Ala^1 and Ala^3–Ala^4 peptide bonds, which exhibit *trans*-peptide bonds. The plane of the Ala^5–D-Ala^1 peptide bond in **11** has rotated by about 170° and in **26** by about 30° in comparison to **16**. Considering the Ala^3–Ala^4 peptide bond, the preferred orientation of the non *N*-methylated peptide bond is observed in **11**, however, the *N*-methylation of the Ala^3–Ala^4 peptide bond results in a different conformation of the peptide bond plane twisted by about 110° in **16** as otherwise it would encounter strong steric clash with Ala^3N^{Me} and Ala^4H^{β}. This orientation is, however, violated in **26** as the *N*-methylation of Ala^5–D-Ala^1 peptide bond leads to a strong D-Ala^1N^{Me}–Ala^4N^{Me} steric clash and this eventually reorients the Ala^4N^{Me} which forces the Ala^4–Ala^5 *cis*-peptide bond out providing a room for its spatial orientation. Thus in this series of *N*-methylated cyclic pentaalanine peptides, there is a systematic pattern in the orientation of peptide bond conformation and subsequently the side chain orientation based upon the site of *N*-methylation.

Systematic modulation of conformation by N-methylation: A clear picture of the conformational change by successive *N*-methylation can be obtained by classifying these peptides by virtue of their sites of *N*-methylation (Figure 11). Starting from compound **2**, *N*-methylation on either side (referring to the *N*-methylated site) results in **6** and **9;** in **9** the D-Ala^1 *N*-methylation is tolerated as the D-Ala^1 NH in **2** points down allowing the insertion of an *N*-methyl group without much deviation from backbone of **2**. In **6**, Ala^3 *N*-methylation leads to strong clash between two *N*-methyl groups eventually leading to Ala^2–Ala^3 *cis*-peptide bond. Extending the *N*-methylation of **6** and **9**, three peptides are obtained of which one is conformationally inhomogeneous. In **24**, Ala^5 *N*-methylation leads to the flip of Ala^4–Ala^5 peptide bond

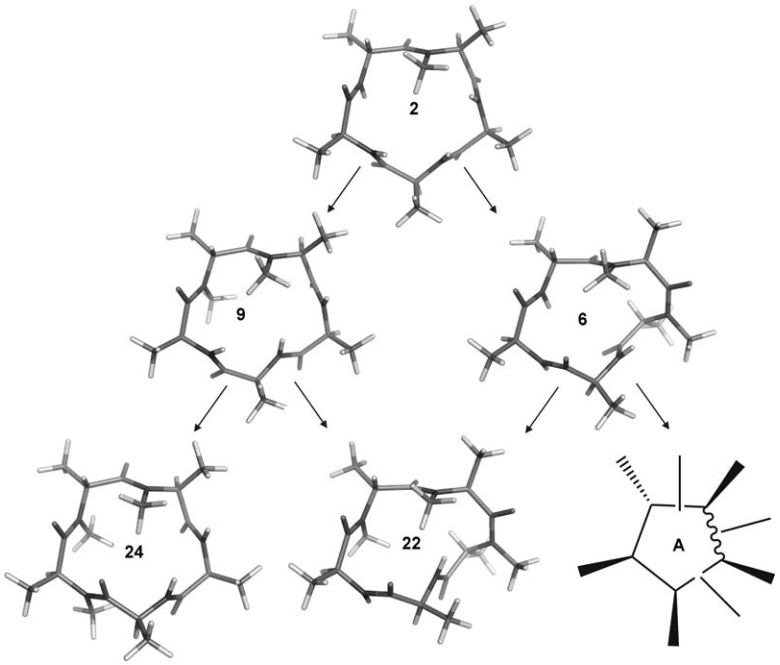

Figure 11. Schematic diagram representing the correlation between the *N*-methylated cyclic peptides obtained by systematic shift and increasing the number of *N*-methylation of cyclo(-D-Ala[1]-MeAla[2]-Ala[3]-Ala[4]-Ala[5]-). "A" shows two different conformation at the NMR spectrum having an abundance of (65:35), therefore the conformational details of this peptide omitted.

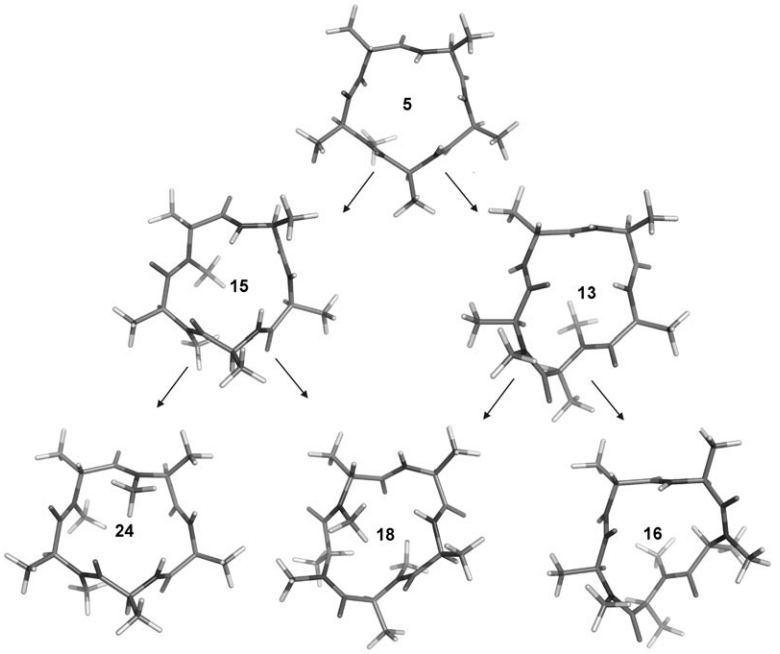

Figure 12. Schematic diagram representing the correlation between the *N*-methylated cyclic peptides obtained by systematic shift and increasing the number of *N*-methyl group of the parent peptide **5** that is, cyclo(-D-Ala[1]-Ala[2]-Ala[3]-Ala[4]-MeAla[5]-).

preferring a *trans* conformation. In **22**, the backbone conformation is not much deviated from that of **6**, as D-Ala[1] *N*-methylation in **6** is sterically allowed.

N-Methylation on either side of **5** results in **15** and **13**. As shown in **24** (Figure 12), *N*-methylation of D-Ala[1] and Ala[5] is tolerated in **15** without enforcing a *cis*-peptide bond conformation. *N*-Methylation of Ala[4] in **5** would have a strong clash with Ala[3] and Ala[4] methyl group, resulting in the 180° flip of Ala[3]–Ala[4] peptide bond (data not presented), which eventually forces the Ala[4]–Ala[5] peptide bond into *cis* conformation. Further *N*-methylation of **13** and **15** leads to **16**, **18** and **24**; in **16**, Ala[3] *N*-methylation introduces *cis*-peptide bond as in **6** and in **18** D-Ala[1] *N*-methylation retains the backbone conformation as **13** with a minor change in the Ala[5]–D-Ala[1] peptide bond plane.

Similarly extending *N*-methylation on either side of **1** (Figure 13) results in **9** and **15**. Further *N*-methylation results in **18**, **22** and **24** which are discussed above. Ala[3] *N*-methylation of **18** leads to **26**, introducing an Ala[2]–Ala[3] *cis* peptide resulting in a similar backbone conformation as **16**, however, the flip of the Ala[3]–Ala[4] peptide bond is noticeable which results from the steric clash of D-Ala[1] *N*-methyl which always points down the plane.

Thus, based on the conformations of all the 15 peptides with a preferred conformation we can summarize the results which are depicted in Table 3.

Finally based on these results, we can predict the preferred orientation of the *N*-methylated peptide bonds in Figure 14. *N*-Methylation at D-Ala[1] and Ala[2] results only in subtle changes in the Φ and Ψ but *N*-methylation at Ala[4] and Ala[5] results in $\approx$180° flip of the respective peptide bond plane in comparison to the parent peptide bond and *N*-methylation only at Ala[3] results in a *cis*-peptide bond.

Conclusion

The conformation of eight *N*-methylated cyclic peptides preferring a major conformation resulting from the parent peptide cyclo(-D-Ala-Ala_4-) are described in detail. These peptides are compared with our previous results of conformationally homogeneous peptides obtained from the same library. With this correlation we have developed a systematic pattern of the impact of *N*-methylation on the backbone conformation of these cyclic peptides.

Thus from these results one can conclude that in cyclic *N*-methylated pentapeptides with the general formula c(aA_4), the region from Ala^5–Ala^3 is strongly preferred and is not possible to introduce a *cis*-peptide bond by variation of the sites or number of *N*-methylations. In contrast, the other side of the cyclic peptide, from Ala^3–Ala^5, is variable and there are possibilities to introduce *cis*-peptide bonds by variation in the pattern and number of *N*-methylation sites.

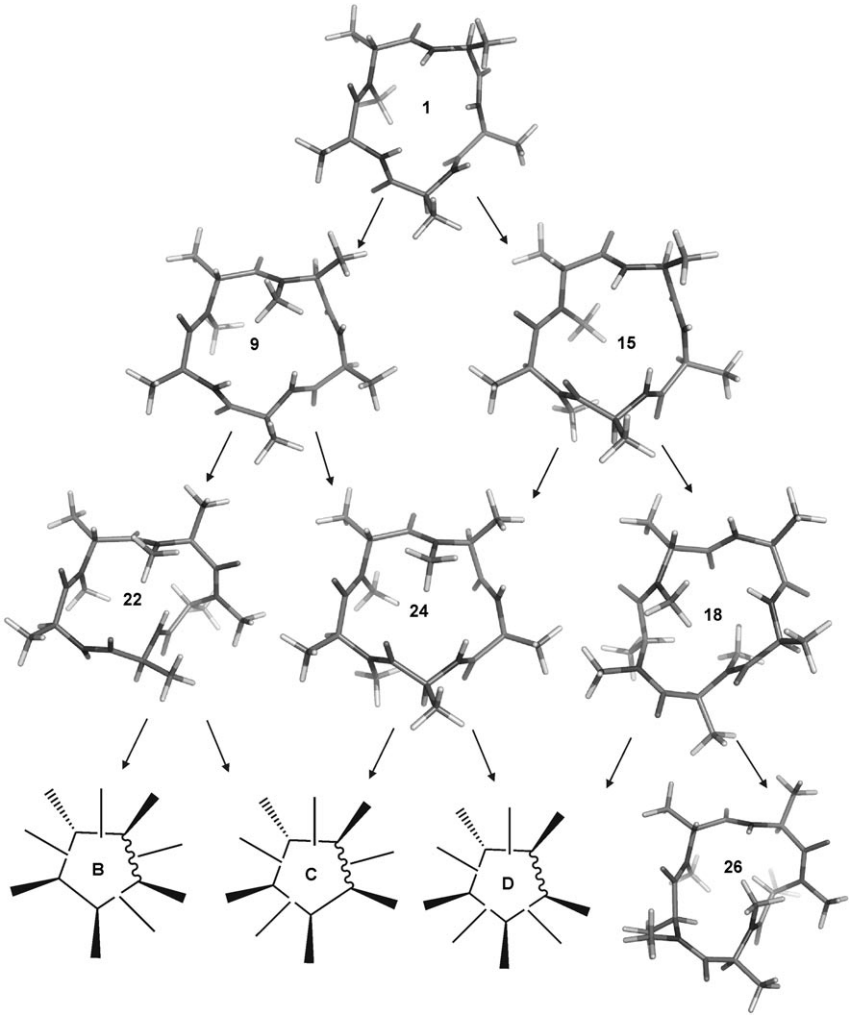

Figure 13. Schematic diagram representing the correlation between the *N*-methylated cyclic peptides obtained by extending the pattern and number of *N*-methylation of the parent peptide cyclo(-D-$MeAla^1$-Ala^2-Ala^3-Ala^4-Ala^5-). Owing to conformational inhomogeneity, the conformations of **B**, **C** and **D** are omitted.

Table 3. c(aA_4) with various patterns of *N*-methylation; numbering refers to the corresponding peptide bond which is *N*-methylated.

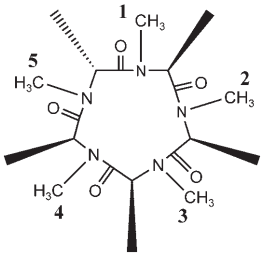

Peptide bond	Conformation
1	always *trans*-
2	always *cis*-
3	always *trans* except **7** (*cis*)
4	*trans*- preferred but *cis*- when 2 and/or 3 *N*-methylated
5	always *trans*-

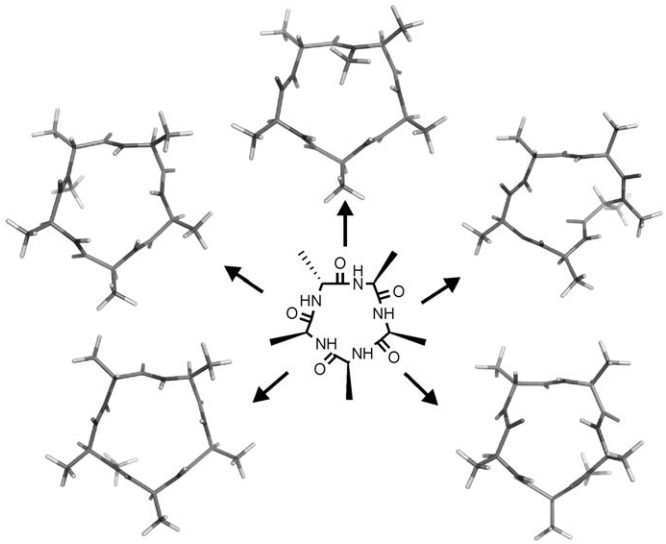

Figure 14. Preferred orientation of the mono *N*-methylated peptide bonds (it should be kept in mind that under sterically demanding conditions, the plane of the peptide bonds Ala^3–Ala^4 and Ala^4–Ala^5 can rotate).

Experimental Section

Synthesis of the cyclic peptides: *N*-Methylalanine was synthesized as described by Freidinger et al.[17] All linear peptides were synthesized using standard Fmoc solid-phase strategy at an *o*-chlorotrityl chloride resin.[18] Non-methylated or *N*-methylated alanine was taken as the C-terminal amino acid, however, the yields were lower in case of a C-terminal *N*-methylated alanine because of endopeptolysis[3c,19] which occurs, when *N*-methylated amino acids or proline are in position one from the resin. Fmoc-deprotection was achieved with 20 vol% piperidine in NMP and the other amino acids (2 equiv each) were sequentially coupled with 2 equiv of 2-(1*H*-benzotriazol-1-yl)-1,1,3,3-tetramethyluronium tetra-fluoroborate (TBTU)[20] and 1-hydroxybenzotriazole (HOBt) in 1-methyl-2-pyrrolidinone (NMP) as the solvent. *N*,*N*-Diisopropylethylamine (DIEA) was used to adjust the pH to 8. In case of coupling to a *N*-methylated residue two equivalents each of *N*-methylalanine or alanine, *N*-[(dimethylamino)-1*H*-1,2,3-triazolo[4,5-*b*]pyridine-1-yl-methylene]-*N*-methylmethanaminium hexafluorophosphate (HATU)[21] and 1-hydroxy-7-azabenzotriazole (HOAt)[22] were used along with DIEA to maintain pH of 8 in NMP as solvent. Due to HOBt/HOAt and HBF_4 formation, the pH drops while the reaction proceeds, leading to reduced nucleophilicity of the amino group. Therefore in the case of insufficient couplings, monitored by the Kaiser test,[23] additional base was added, but the pH was not allowed to exceed a value of 8.5. The coupling time ranged from 20 to 45 min. The *o*-chlorotrityl linker allows to cleave off the linear peptide with a mild treatment of acetic acid/2,2,2-trifluoroethanol (TFE) mixture in CH_2Cl_2 or by using a 20% solution of HFIP (hexafluoroisopropanol) in CH_2Cl_2 without affecting the peptide bonds. The head-to-tail cyclization was performed with diphenylphosphorylacid azide (DPPA),[24] applying the solid base method using $NaHCO_3$ in *N*,*N*-dimethylformamide (DMF). After the completion of cyclization, which was monitored by ESI mass spectroscopy, DMF was evaporated and the peptide was redissolved in minimum amount of dry acetonitrile, which precipitated the cyclization reagents and left the crude product dissolved in acetonitrile. The pure compound was obtained by reversed phase high-performance liquid chromatography (RP-HPLC) purification (see Supporting Information in ref. [1c] for yields). The peptides were characterized by ESI mass and various NMR techniques.

NMR Spectroscopy: All spectra were recorded at 297 K on a 500 MHz Bruker DMX spectrometer (Bruker, Karlsruhe, Germany), in [D$_6$]DMSO (^{1}H, 2.49 ppm; ^{13}C 39.5 ppm) and were processed using XWINNMR (Bruker) and analyzed with either XWINNMR or SPARKY.[25] The assignment of all proton and carbon resonances followed the standard strategy as previously described.[26] Sequential assignment was accomplished by through-bond connectivity's from heteronuclear multiple bond correlation (HMBC)[27] spectrum. The *N*-methyl group was taken as the reference for the sequence assignment, the protons of which show a correlation with the ^{13}C shift of the intra-residual β-methyl group by a four bond coupling at the HMBC spectrum. The β-methyl protons further show a correlation with the ^{13}C shift of intra-residual carbonyl by a three bond coupling, and this carbonyl also correlates with the H^{α} shift of the same residue and the H^{N} shift of the adjacent residue (if not *N*-methylated) by a strong two bond coupling. In this way the full sequence assignment was accomplished. TOCSY spectra were recorded with a mixing time of 60 ms and ROESY spectra with a mixing time of 150 ms. Temperature coefficients for the amide protons of each peptide were determined via one-dimensional spectra in the range from 297 to 327 K with a step size of 5 K. Many of these compounds show more than one conformation in slow exchange on the NMR time scale at room temperature. Chemical exchange were proven by ROESY spectra, which show inverted sign as signals caused by ROEs.[28]

Computational methods: Proton distances were calculated according to the isolated two-spin approximation from volume integrals of rotating frame nuclear Overhauser enhancement (ROESY)[29] spectra. The integrated volume of the ROE cross peaks were offset corrected[30] and converted to proton–proton distance employing cross peak intensity of H^{α}–H^{β} of alanine as reference (2.19 Å). Restraints were obtained by adding and subtracting 10% to the calculated experimental distances, accounting for errors via the two-spin approximation, cross-peak integration and the slight variation of ROE due to spin diffusion. Metric matrix DG calculations were carried out with a home-written program utilizing random metrization.[31] Experimental distance constraints which were more restrictive than the geometric distance bounds (holonomic restraints) were used to create the final distance matrix. The structures were first embedded in four dimensions and then partially minimized using conjugate gradients followed by distance-driven dynamics (DDD);[32] wherein only distance constraints were used. The DDD simulation was carried out at 1000 K for 50 ps with a gradual reduction in temperature over the next 30 ps. The DDD procedure utilized holonomic and experimental distance constraints plus a chiral penalty function for the generation of the violation "energy" and forces. A distance matrix was calculated from each structure, and the EMBED algorithm was used to calculate coordinates in three dimensions. About 95–100 structures were calculated for each peptide, and >90% of the structures of every peptide didn't show any significant violation. The MD calculations were carried out with the program DISCOVER using the CVFF force field.[33] The structure resulting from DG calculation was placed in a cubic box of length 25 Å and soaked with DMSO and a restrained MD simulation was carried out. After energy minimization using steepest descent and conjugate gradient, the system was heated gradually starting from 10 K and increasing to 50, 100, 150, 200, 250 and 300 K in 2 ps steps, each by direct scaling of velocities. The system was equilibrated for 50 ps with temperature bath coupling (300 K). Configurations were saved every 100 fs for another 150 ps. Finally a 150 ps free MD simulation at 300 K was carried out to prove that the stability of the calculated conformation in the solvent is similar to the structure obtained from experimental restraints.

Acknowledgements

The authors gratefully acknowledge technical assistance from Burkhard Cordes. We thank the Humboldt foundation for the generous support via the Max-Planck-Forschungspreis.

[1] a) H. Kessler, *Angew. Chem.* **1982**, *94*, 509–520; *Angew. Chem. Int. Ed. Engl.* **1982**, *21*, 512–523; b) D. F. Mierke, M. Kurz, H. Kessler, *J. Am. Chem. Soc.* **1994**, *116*, 1042–1049; c) J. Chatterjee, D. Mierke, H. Kessler, *J. Am. Chem. Soc.* **2006**, *128*, 15164–15172.

[2] a) H. Kessler, R. Gratias, G. Hessler, M. Gurrath, G. Müller, *Pure Appl. Chem.* **1996**, *68*, 1201–1205; b) R. Haubner, R. Gratias, B. Diefenbach, S. L. Goodman, A. Jonczyk, H. Kessler, *J. Am. Chem. Soc.* **1996**, *118*, 7461–7472.

[3] a) D. F. Veber, R. Saperstein, R. F. Nutt, R. M. Freidinger, S. F. Brady, P. Curley, D. S. Perlow, W. J. Paleveda, C. D. Colton, A. G. Zacchei, D. J. Tocco, D. R. Hoff, R. L. Vandlen, J. E. Gerich, L. Hall, L. Mandarino, E. H. Cordes, P. S. Anderson, R. Hirschmann, *Life Sci.* **1984**, *34*, 1371–1378; b) A. C. Bach, C. J. Eyermann, J. D. Gross, M. J. Bower, R. L. Harlow, P. C. Weber, W. F. Degrado, *J. Am. Chem. Soc.* **1994**, *116*, 3207–3219; c) M. Teixido, F. Albericio, E. Giralt, *J. Pept. Res.* **2005**, *65*, 153–166; d) C. Gilon, M. A. Dechantsreiter, F. Burkhart, A. Friedler, H. Kessler, in H *ouben-Weyl Methods of Organic Chemistry. Vol E22c: Synthesis of Peptides and Peptidomimetics* (Eds.: M. Goodman, A. Felix, L. Moroder, C. Tonolio), Thieme, Stuttgart (Germany), **2002**, pp. 215-291 and references therein.

[4] Y. Takeuchi, G. R. Marshall, *J. Am. Chem. Soc.* **1998**, *120*, 5363–5372.

[5] a) M. Altstein, O. Ben-Aziz, S. Daniel, I. Schefler, I. Zeltser, C. Gilon, *J. Biol. Chem.* **1999**, *274*, 17573–17579; b) M. A. Dechantsreiter, E. Planker, B. Mathä, E. Lohof, G. Hölzemann, A. Jonczyk, S. L. Goodman, H. Kessler, *J. Med. Chem.* **1999**, *42*, 3033–3040.

[6] a) F. Piriou, K. Lintner, S. Fermandjian, P. Fromageot, M. C. Khosla, R. R. Smeby, F. M. Bumpus, *Proc. Natl. Acad. Sci. USA* **1980**, *77*, 82–86; b) A. E. Tonelli, *Biopolymers* **1976**, *15*, 1615–1622; c) D. J. Patel, A. E. Tonelli, *Biopolymers* **1976**, *15*, 1623–1635.

[7] H. Kessler, *Angew. Chem.* **1970**, *82*, 237–253; *Angew. Chem. Int. Ed. Engl.* **1970**, *9*, 219–235.
[8] W. G. Rajeswaran, S. J. Hocart, W. A. Murphy, J. E. Taylor, D. H. Coy, *J. Med. Chem.* **2001**, *44*, 1305–1311.
[9] D. J. Gordon, R. Tappe, S. C. Meredith, *J. Pept. Res.* **2002**, *60*, 37–55.
[10] W. L. Cody, J. X. He, M. D. Reily, S. J. Haleen, D. M. Walker, E. Reyner, B. H. Stewart, A. M. Doherty, *J. Med. Chem.* **1997**, *40*, 2228–2240.
[11] a) W. G. Rajeswaran, S. J. Hocart, W. A. Murphy, J. E. Taylor, D. H. Coy, *J. Med. Chem.* **2001**, *44*, 1416–1421; b) J. Erchegyi, C. A. Hoeger, W. Low, D. Hoyer, B. Waser, V. Eltzschinger, J. C. Schaer, R. Cescato, J. C. Reubi, J. E. Rivier, *J. Med. Chem.* **2005**, *48*, 507–514.
[12] J. P. Snyder, *J. Am. Chem. Soc.* **1984**, *106*, 2393–2400.
[13] M. Heller, M. Sukopp, N. Tsomaia, M. John, D. F. Mierke, B. Reif, H. Kessler, *J. Am. Chem. Soc.* **2006**, *128*, 13806–13814.
[14] V. F. Bystrov, V. T. Ivanov, S. L. Portnova, T. A. Balashov, Y. A. Ovchinni, *Tetrahedron* **1973**, *29*, 873–877.
[15] H. Kessler, C. Griesinger, J. Lautz, A. Müller, W. F. Van Gunsteren, H. J. C. Berendsen, *J. Am. Chem. Soc.* **1988**, *110*, 3393–3396.
[16] B. Keller, M. Christen, C. Oostenbrink, W. F. van Gunsteren, *J. Biomol. NMR* **2007**, *37*, 1–14.
[17] R. M. Freidinger, J. S. Hinkle, D. S. Perlow, B. H. Arison, *J. Org. Chem.* **1983**, *48*, 77–81.
[18] a) K. Barlos, D. Gatos, J. Kallitsis, G. Papaphotiu, P. Sotiriu, W. Q. Yao, W. Schafer, *Tetrahedron Lett.* **1989**, *30*, 3943–3946; b) K. Barlos, O. Chatzi, D. Gatos, G. Stavropoulos, *Int. J. Pept. Protein Res.* **1991**, *37*, 513–520.
[19] M. J. O. Anteunis, C. Vanderauwera, *Int. J. Pept. Protein Res.* **1988**, *31*, 301–310.
[20] R. Knorr, A. Trzeciak, W. Bannwarth, D. Gillessen, *Tetrahedron Lett.* **1989**, *30*, 1927–1930.
[21] a) L. A. Carpino, A. El-Faham, C. A. Minor, F. Albericio, *Chem. Commun.* **1994**, 201–203; b) F. Albericio, J. M. Bofill, A. El-Faham, S. A. Kates, *J. Org. Chem.* **1998**, *63*, 9678–9683.
[22] L. A. Carpino, *J. Am. Chem. Soc.* **1993**, *115*, 4397–4398.
[23] E. Kaiser, R. L. Colescot, C. D. Bossinge, P. I. Cook, *Anal. Biochem.* **1970**, *34*, 595–598.
[24] a) T. Shioiri, S. Yamada, K. Ninomiya, *J. Am. Chem. Soc.* **1972**, *94*, 6203–6205; b) S. F. Brady, S. L. Varga, R. M. Freidinger, D. A. Schwenk, M. Mendlowski, F. W. Holly, D. F. Veber, *J. Org. Chem.* **1979**, *44*, 3101–3105; c) S. F. Brady, W. J. Paldeva, B. H. Arison, R. M. Freidinger, R. F. Nutt, D. F. Veber, in *8th Annual Peptide Symposium* (Eds.: V. J. Hruby, D. H. Rich), Pierce Chemical, Rockford, IL (USA), **1983**, pp. 127–130.
[25] T. D. Goddard, D. G. Kneller, SPARKY 3, University of California, San Francisco (USA).
[26] H. Kessler, W. Schmitt, in *Encyclopedia of Nuclear Magnetic Resonance* (Eds.: D. M. Grant, R. K. Harris), Wiley, New York, **1995**.
[27] A. Bax, M. F. Summers, *J. Am. Chem. Soc.* **1986**, *108*, 2093–2094.
[28] H. Kessler, M. Gehrke, C. Griesinger, *Angew. Chem.* **1988**, *100*, 507–554; *Angew. Chem. Int. Ed. Engl.* **1988**, *27*, 490–536.
[29] a) A. A. Bothnerby, R. L. Stephens, J. M. Lee, C. D. Warren, R. W. Jeanloz, *J. Am. Chem. Soc.* **1984**, *106*, 811–813; b) H. Kessler, C. Griesinger, R. Kerssebaum, K. Wagner, R. R. Ernst, *J. Am. Chem. Soc.* **1987**, *109*, 607–609.
[30] a) C. Griesinger, R. R. Ernst, *J. Magn. Reson.* **1987**, *75*, 261–271; b) A. Bax, *J. Magn. Reson.* **1988**, *77*, 134–147.
[31] T. F. Havel, *Prog. Biophys. Mol. Biol.* **1991**, *56*, 43–78.
[32] a) D. F. Mierke, R. M. Scheek, H. Kessler, *Biopolymers* **1994**, *34*, 559–563; b) D. F. Mierke, A. Geyer, H. Kessler, *Int. J. Pept. Protein Res.* **1994**, *44*, 325–331.
[33] a) A. T. Hagler, S. Lifson, P. Dauber, *J. Am. Chem. Soc.* **1979**, *101*, 5122–5130; b) D. F. Mierke, H. Kessler, *J. Am. Chem. Soc.* **1991**, *113*, 9466–9470.

Received: July 4, 2007
Published online: December 13, 2007

